Int. J. Environ. Sci. Technol. (2016) 13:1861–1872
DOI 10.1007/s13762-016-1026-z

ORIGINAL PAPER

Phosphorylated nanocellulose papers for copper adsorption from aqueous solutions

A. Mautner[1,2] · H. A. Maples[1] · T. Kobkeatthawin[1,3] · V. Kokol[4] · Z. Karim[5] · K. Li[6] · A. Bismarck[1,2]

Received: 9 December 2015 / Revised: 23 March 2016 / Accepted: 18 May 2016 / Published online: 2 June 2016

Abstract Copper is a major problem in industrial wastewater streams, seriously affecting the quality of potential drinking water. Several approaches, including continuous membrane processes or batch-wise application of adsorbents, are in use to tackle this problem. Unfortunately, these processes suffer from their particular drawbacks, such as low permeance or disposal of saturated adsorbents. However, a combination of these processes could constitute a step towards a more efficient copper removal solution. Here, we present a nanopaper ion-exchanger prepared from cellulose nanofibrils produced from fibre sludge, a paper industry waste stream, for the efficient, continuous removal of copper from aqueous solutions. This nanopaper ion-exchanger comprises phosphorylated cellulose nanofibrils that were processed into nanopapers by papermaking. The performance of these phosphorylated nanopaper membranes was determined with respect to their rejection of copper and permeance. It was shown that this new type of nanopaper is capable of rejecting copper ions during a filtration process by adsorption. Results suggest that functional groups on the surface of the nanopapers contribute to the adsorption of copper ions to a greater extent than phosphate groups within the bulk of the nanopaper. Moreover, we demonstrated that those nanopaper ion-exchangers could be regenerated and reused and that in the presence of calcium ions, the adsorption capacity for copper was only slightly reduced.

Keywords Cellulose nanofibrils · Heavy metal ion · Ion-exchange · Phosphorylation

✉ A. Mautner
andreas.mautner@univie.ac.at

[1] Polymer and Composite Engineering (PaCE) Group, Institute for Materials Chemistry and Research, University of Vienna, Währingerstr. 42, 1090 Vienna, Austria

[2] Polymer and Composite Engineering (PaCE) Group, Department of Chemical Engineering, Imperial College London, South Kensington Campus, London SW7 2AZ, UK

[3] Department of Chemistry and Center of Excellence for Innovation in Chemistry, Faculty of Science, Prince of Songkla University, Songkhla 90110, Thailand

[4] Institute for Engineering Materials and Design, Faculty of Mechanical Engineering, University of Maribor, 2000 Maribor, Slovenia

[5] Division of Materials Science, Department of Engineering Sciences and Mathematics, Luleå University of Technology, 97187 Luleå, Sweden

[6] Department of Chemical Engineering, Imperial College London, South Kensington Campus, London SW7 2AZ, UK

Introduction

Copper is one of the most utilized heavy metals in many different industries found in a wide range of different applications (Camarillo et al. 2010). In 2014, the world's copper consumption equalled 20.6 million short tons (C.D.A. 2015). This is due to its excellent properties (Lambert et al. 2014), such as very good electrical and thermal conductivity, ductility and availability (Samuelsson and Björkman 2014). Contamination of drinking water can occur during mining and production processes, where copper ions leak into water streams and are further distributed (Akar et al. 2009; Bilal et al. 2013). Apart from traditional applications, copper is also used as fungicide or fertilizer for plants and as nutrient supplement for animals, resulting in accumulation of copper in manure, ultimately causing soil contamination and thus contamination of

drinking water sources (Tegoni et al. 2014). Potential sources of copper in industrial effluents also include pulp, paper and paper board mills as well as the fertilizer industry (Gupta 1998; Wan Ngah et al. 2002).

Even though copper is essential for the human body (Fraga 2005; Bilal et al. 2013), high copper concentrations are a serious problem (Shannon et al. 2008), as it causes adverse effects in living organisms, e.g. the accumulation of copper in the liver roots Wilson's disease, which leads to neurological and psychiatric defects (Araya et al. 2001; Zamani et al. 2007). The necessary intake of copper for humans should not exceed 5 mg per day, as defined by the tolerable upper intake level (UL), set by the European Commission (European-Comission 2003). Thus, according to the WHO (WHO 2004), the limit of copper concentration in water should not exceed 2 mg L^{-1}, which is often exceeded in many industrialized regions. On the other hand, due to increased prices for raw metals such as copper, the capture of copper from waste streams, and thus the recycling of this precious material, is not only important from an ecological but also interesting from an economical point of view (Samuelsson and Björkman 2014).

Currently, high copper concentrations in water are usually tackled by various methods and processes, for instance by chemical precipitation (Chen et al. 2009; Fu and Wang 2011), e.g. hydroxide, sulphide or chelating precipitation, as well as ion-exchange or adsorption (Wan Ngah et al. 2002; Akar et al. 2009; Zhu and Li 2015; Jain et al. 2016), e.g. with activated carbon, carbon nanotubes, magnetic nanoparticles (Feitoza et al. 2014), low-cost adsorbents from industrial waste streams (Castaldi et al. 2015; Cretescu et al. 2015) or bioadsorbents (Davis et al. 2003; Deng et al. 2013; Hokkanen et al. 2013; Shaheen et al. 2013; Bansal et al. 2014; Şen et al. 2015; Komkiene and Baltrenaite 2016). Furthermore, membrane filtration processes (Ujang and Anderson 1996; Qdais and Moussa 2004) such as ultrafiltration, nanofiltration, reverse osmosis or electrodialysis are utilized. Coagulation, flocculation, flotation (Fu and Wang 2011) as well as electrochemical treatment (Kongsricharoern and Polprasert 1995; Huang et al. 2014) are also among those processes. Unfortunately, all of these methods and processes exhibit drawbacks that limit their utility. Membrane processes are usually connected to process complexity, membrane fouling and low permeate flux; coagulation–flocculation involves chemical consumption and sludge generation; and flotation causes high initial capital, maintenance and operational costs (Ujang and Anderson 1996; Qdais and Moussa 2004). Chemical precipitation is often not economically feasible and produces large amounts of sludge; ion-exchange resins are often expensive and have to be regenerated, causing serious secondary pollution; and the development of electrochemical heavy metal wastewater treatment techniques is restricted due to high initial capital investment and expensive electricity supply (Kongsricharoern and Polprasert 1995; Akar et al. 2009). The use of activated carbons for the adsorption of heavy metal ions is restricted due to its high cost (Fu and Wang 2011), while utilization of low-cost adsorbents is often limited by their adsorption efficiencies (Cretescu et al. 2015; Komkiene and Baltrenaite 2016). However, biosorption of heavy metals from aqueous solutions, adsorption of contaminants on adsorbents based on renewable resources, is a relatively new process that has proved very promising for the removal of heavy metals from wastewater (Shaheen et al. 2013; Mejias Carpio et al. 2014).

Cellulose nanofibrils (CNF), a special type of cellulose with fibrils in the nm range (Klemm et al. 2011), were recently demonstrated to be capable of removing different kinds of ions by adsorption in static media whereby via the introduction of certain functional groups, such as acid or ammonium groups, the effect of adsorption of heavy metal ions, dyes or nitrates can be enhanced to a great extent (Hokkanen et al. 2013; Jin et al. 2013; Pei et al. 2013; Yu et al. 2013a, b; Karim et al. 2014; Liu et al. 2014; Sehaqui et al. 2014). CNF can be produced from industrial waste streams, for example fibre sludge, and do not necessarily require chemicals or solvents for their production. Thus, a material from a renewable resource is at hand which has the capacity to adsorb pollutants from aqueous solutions (Klemm et al. 2011; Jonoobi et al. 2012). Phosphate-modified CNF were recently shown to be particularly suitable as adsorbent for heavy metals (Božič et al. 2014; Liu et al. 2015). Anyhow, the problems associated with adsorbent materials, e.g. batch-wise application, non-continuous operation (Bhatnagar and Sillanpää 2011), have also to be tackled for these CNF adsorbents.

Apart from application as adsorbent, CNF can also be utilized for manufacturing of nanopapers, using paper-making processes (Henriksson et al. 2008; Sehaqui et al. 2010; Lee et al. 2012). Such nanopapers can be used as tight aqueous ultrafiltration or organic solvent nanofiltration membranes (Mautner et al. 2014, 2015). However, the permeance of these membranes was still relatively low and pores too large for the removal of (copper) ions. Moreover, for the adsorption of heavy metal ions conventional nanopapers lack suitable amounts of functional groups, such as phosphate groups.

In this study, our approach was to combine the advantages of a natural adsorbent material and membrane filtration processes. We prepared phosphorylated cellulose nanofibrils using fibre sludge, a paper industry waste stream, as cheap and abundant raw material. These phosphorylated CNF were processed into nanopaper ion-exchangers to capture copper ions in a filtration process. The advantage of this approach is that it constitutes a continuous process, and thus, adsorbent material disposal problems are avoided, as backwash operations can be easily performed as shown in our paper. The development of an adsorbent into a continuously working nanopaper ion-exchanger represents a step forward in tackling the problem of heavy metal, i.e. copper, accumulation in water resources.

The production of cellulose nanofibrils was conducted in spring 2014 at Lulea University, and the phosphorylation of the cellulose nanofibrils was carried out in spring 2014 by the University of Maribor. Preparation of the nanopapers was done in summer 2014 at Imperial College London, and the testing of the nanopapers was performed in summer and autumn 2014 at Imperial College London as well as in summer 2015 and winter 2015/16 at the University of Vienna.

Materials and methods

Materials

H_3PO_4, $Cu(NO_3)_2$, KOH, NaOH, HCl and KCl were purchased from Sigma and used without further purification. For permeance measurements, deionized water was used which was further purified with a UV unit (Synergy Millipore, Molsheim, France).

Preparation of unmodified CNF

Unmodified nanofibrils were prepared according to a process previously reported (Jonoobi et al. 2012) from fibre sludge, which had a cellulose and hemicellulose content of 95 and 4.75 %, respectively, and was kindly provided by Processum AB (Domsjö, Sweden). Briefly, the sludge raw material was immersed in distilled water at a consistency of 3 wt% for 2 h and then dispersed using a mechanical blender (Silverson L4RT, Chesham Bucks, England) at 3000 rpm for 10 min. Subsequently, unmodified nanofibrils, herein termed CNF-0, were obtained by grinding the suspension with an ultrafine grinder (MKCA 6-3, Masuko Sangyo, Kawaguchi, Japan).

Preparation of phosphorylated CNF

To a CNF-0 suspension in water (3.0 wt%), H_3PO_4 (85 vol%) was carefully (keeping the temperature below 30 °C) added via a dropping funnel to reach a H_3PO_4 concentration of 10.7 mol L^{-1}. Afterwards, the reaction mixture was heated to 100 °C in an oil bath and stirred for 30 min, and subsequently the slightly yellow-coloured reaction mixture was cooled to room temperature in an ice bath. Phosphorylated CNF (CNF-P) were collected by centrifuging ten times at 9000 rpm for 15 min until the supernatant was clear. After each pass, the supernatant was decanted and replaced by fresh ultrapure water. The CNF-P dispersion was then dialysed (the weight cut-off of the dialysis membrane was 6–8 kDa) against ultrapure water for 5 days (exchanging the water every day) until neutral pH was reached. The final dispersion was subsequently sonicated for 2 min and stored in a refrigerator.

Characterization of phosphorylated CNF

Determination of the Zeta-potential of CNF

The ζ-potential of CNF was measured using electrophoresis with a Zeta-sizer (Malvern Nano ZS, Malvern, Herrenberg, Germany) at 20 °C using a high concentration zeta-potential cell (ZEN1010). A voltage of 40 V was applied across the nominal electrode spacing of 16 mm. Samples were prepared at concentrations of 0.005 wt% in MQ water and measured over a pH range from 12.5 to 2 by titration of 0.1 mol L^{-1} NaOH and 0.1 mol L^{-1} HCl, respectively. The samples were ultrasonicated and stirred for 2 min prior to the measurements in order to improve particle dispersion. Mean values ± standard deviations were calculated from at least four individual measurements.

Phosphate content by potentiometric titration

Potentiometric titrations with 0.5 wt% suspensions of the phosphorylated CNF in water were performed using a twin-burette instrument Mettler-Toledo T70 (Mettler-Toledo, Ljubljana-Dobrunje, Slovenia) under inert atmosphere (N_2 bubbling) as reported before (Liu et al. 2015). Briefly, suspensions of CNF and acidic or alkali solutions, respectively, were prepared in MQ water with low carbonate content ($<10^{-5}$ mol L^{-1}). The titration experiments were carried out at 0.1 mol L^{-1} ionic strength, as set with KCl. The pH value was measured with a Mettler-Toledo

DG-117 combined glass electrode. Blank titration was carried out under the same conditions.

The total amount of phosphate groups per unit mass CNF Γ_Q (mmol g^{-1}) was determined from the volume of KOH added for the CNF sample, from which the volume of the blank was deducted, according to Eq. 1:

$$\Gamma_Q = \frac{V}{m}([Cl^-] - [K^+] + [OH^-] - [H^+]) \quad (1)$$

whereby m is the mass of CNF and V is the corrected volume of KOH used. The values in the square brackets denote the molar concentrations of the ionic species: $[Cl^-]$ and $[K^+]$ are known from the added volumes of HCl and KOH, respectively, and $[OH^-]$ and $[H^+]$ are known from the measured pH.

Manufacturing of nanopapers

Nanopapers were prepared following a protocol reported previously (Hasani et al. 2008; Sehaqui et al. 2010; Lee et al. 2012). Initially, the concentration of CNF was adjusted to 0.3 wt% by adding water. Subsequently, these CNF-in-water suspensions were blended (Breville VBL065-01, Oldham, UK) for 2 min to obtain a homogeneous suspension, followed by vacuum filtration onto a cellulose filter paper (VWR 413, Lutterworth, UK) to produce a filter cake. The resulting filter cakes were wet-pressed (10 kg) between blotting papers (3MM Chr VWR, Lutterworth, UK) for 5 min to further absorb the excess water, ultimately exhibiting a moisture content of 85 %. Consolidation and drying of the filter cakes were conducted in a hot-press (25-12-2H, Carver Inc., Wabash, USA) (1 t, 1 h, 120 °C) by sandwiching between fresh blotting papers and metal plates. CNF-P and CNF-0 nanopapers with 25 g m^{-2} (gsm), corresponding to thicknesses of 25 µm, were prepared.

By mixing and blending equal amounts of CNF-0 and CNF-P, respectively, at 0.3 wt%, suspensions for the production of hybrid nanopapers (CNF-H), which consisted of equimolar mixtures of modified and unmodified CNF, were prepared, followed by filtering, pressing and hot-pressing as described above. CNF-H nanopapers with 50 (gsm), which were composed of each 25 gsm CNF-P and 25 gsm CNF-0, with a thickness of 50 µm were prepared, containing the same amount of phosphate groups as 25 gsm CNF-P nanopapers.

Moreover, a double-layer nanopaper (CNF-P top) with a 40 gsm CNF-0 substrate and a 10 gsm active CNF-P top layer was produced. It was prepared by first filtering a CNF-0 suspension onto which a CNF-P suspension was casted. The double-layer wet filter cake was finally pressed and hot-pressed as described above.

Characterization of nanopapers

Determination of the Zeta-potential of nanopapers

The ζ-potential of CNF-0, CNF-P (top) and CNF-H nanopapers was determined with a SurPASS electrokinetic analyser from Anton Paar (Graz, Austria). The ζ-potential was measured as a function of pH in an adjustable gap cell (gap width 100 µm) by pumping the electrolyte solution (1 mM KCl) through the cell and steadily increasing the pressure to 300 mbar, while the pH was controlled by titrating 0.05 mol L^{-1} KOH and 0.05 mol L^{-1} HCl into the electrolyte solution. To determine the ζ-potential, the measured streaming current was used.

Morphology of the cellulose nanopapers by SEM

The morphology of modified and unmodified nanopapers was characterized using scanning electron microscopy (SEM). Prior to SEM, the nanopapers were mounted onto aluminium stubs using carbon tabs and gold coated (K550 sputter coater, Emitech Ltd, Kent, UK) for 2 min at 20 mA. SEM images were taken using a LEO Gemini 1525 FEG-SEM (Leo Electron Microscopy Ltd, Cambridge, UK) at an accelerating voltage of 5 kV.

Mechanical properties of cellulose nanopapers by tensile tests

Tensile properties of the nanopapers were determined using a 5969 Dual Column Universal Testing System (Instron, Darmstadt, Germany) with a 1 kN load cell at 25 °C and 50 % RH with a gauge length of 20 mm and a testing velocity of 1 mm min^{-1}. With a laboratory paper, cutter strips (40 × 5 mm^2) were cut from the nanopapers, whereby the thickness was separately measured for each specimen before measurements at five different spots using a digital micrometre (705-1229, RS components, Corby, UK).

Nanopaper pure water permeance and copper adsorption performance

Two parameters were used to evaluate the performance of the nanopapers: the pure water permeance and copper ion adsorption. To study the permeance, discs of nanopapers with a diameter of 49 mm were soaked in deionized water for three days ensuring equilibration, placed on a porous stainless steel plate and installed in a Sterlitech (Kent, USA) HP4750 stirred dead-end cell with an active filtration area of 1460 mm^2. At a head pressure of 0.2 MPa nitrogen, deionized water was forced through the nanopapers at

20 °C. Measuring the volume permeated per unit area per unit time resulted in values for the pure water permeance [L m^{-2} h^{-1} MPa^{-1}] (Mautner et al. 2016).

To study the copper ion adsorption, 1 mmol L^{-1} solutions of Cu^{2+} ions (from $Cu(NO_3)_2$, pH 5.5) in deionized water were passed through the nanopapers. Permeate fractions of 2–5 mL were collected and diluted by a factor of 3 to enable analysis by ICP-OES (PerkinElmer Optical Emission Spectrometer Optima 2000 DV, Perkin Elmer, Waltham, USA). The mass of adsorbed copper ions per unit nanopaper area [mg m^{-2}] was computed from the volume of each permeate fraction and its concentration and plotted versus the permeate volume. The adsorption capacity, i.e. the ratio of the mass of adsorbed copper to the total mass of phosphorylated CNF [mg g^{-1}], was calculated from the total mass of adsorbed copper ions. Regeneration of copper loaded nanopapers was demonstrated by washing with 0.1 M H_3PO_4. Washed nanopapers were tested again according to the protocol described above. Furthermore, to evaluate the influence of calcium ions onto the adsorption of copper onto CNF-P nanopapers, dynamic adsorption studies were performed with aqueous solutions containing 1 mmol L^{-1} of each Cu^{2+} and Ca^{2+}, respectively.

Results and discussion

Phosphorylated CNF

Production of CNF-0 from fibre sludge, an industrial waste stream material, resulted in cellulose nanofibrils with diameters between 10 and 100 nm, with the maximum of the diameter distribution being located around 30 nm, and lengths in the µm region (Jonoobi et al. 2012). This base material was used directly for the production of nanopapers as well as for the preparation of phosphorylated CNF-P. The phosphorylation reaction (Kokol et al. 2015) was carried out through esterification of cellulosic OH groups with phosphoric acid at 100 °C, as shown in Scheme 1.

The success of this modification reaction was confirmed by means of potentiometric titration and ζ-potential measurements. The amount of phosphate groups grafted onto the cellulose fibrils, as determined by conductometric titration, was 18.6 ± 2.3 mmol kg^{-1}, which equals an overall degree of substitution (DS) of just 0.001. It can be assumed that the phosphoric acid was attached to the cellulose chain in the form of a phosphate group by one ester bond via the reactions of the cellulose hydroxyl groups (Suflet et al. 2010). The modification reaction led to slight alterations of the fibrils; hydrolysis of fibrils located in amorphous regions of the surface of the CNF took place, resulting in a yield of 85 %. Further in-detail characterization (including IR and SEM before and after modification, NMR, XRD, capillary electrophoresis, colorimetry, DSC and TGA) of the phosphorylated CNF used in this study can be found in a preceding study (Kokol et al. 2015).

The modification of CNF with phosphate groups is anticipated to influence the surface charge of CNF. ζ-Potential measurements (Fig. 1) displayed a significant change in the ζ-potential of the native nanocellulose fibrils due to the CNF modification. Unmodified CNF-0 exhibited a negative ζ-potential over the whole range of pH examined between −2.5 and −21 mV. A plateau around −20 mV at high pH can be observed, which indicates that the surface is acidic as all dissociable functional groups are fully deprotonated (Lee et al. 2012). With decreasing pH, the ζ-potential increases due to the protonation of functional groups. Above pH 4, phosphate-modified CNF-P exhibit negative ζ-potential, too, but on a lower level (−21 to −31 mV). This lower ζ-potential is due to the introduction of acidic phosphate groups on the surface of the nanofibrils eventually improving adsorption of positively charged heavy metal ions, i.e. copper ions (Kokol et al. 2015). However, at pH 2.5, charge reversal and thus a positive ζ-potential of 3 mV was found. Below the isoelectric point (iep), the grafted moieties, present in the form of hydrogen phosphate groups, are protonated, resulting in increased ζ-potential. This is in good correlation with the pK_{a1} value that is 2.1 for phosphoric acid (Guthrie 1977).

Phosphorylated CNF nanopapers

From phosphorylated CNF-P, nanopapers intended for the continuous capture of copper ions via an ion-exchange mechanism were prepared using a papermaking process (Mautner et al. 2014, 2015). The grammage of CNF-P nanopapers was set to 25 g m^{-2} (gsm), corresponding to a thickness of 25 µm. Moreover, a hybrid nanopaper (CNF-H) was prepared, in which CNF-P and CNF-0 were mixed

Scheme 1 Modification of cellulose nanofibrils with phosphate groups

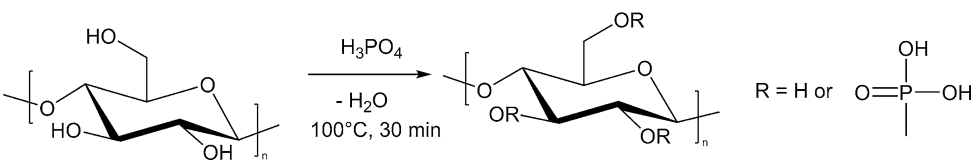

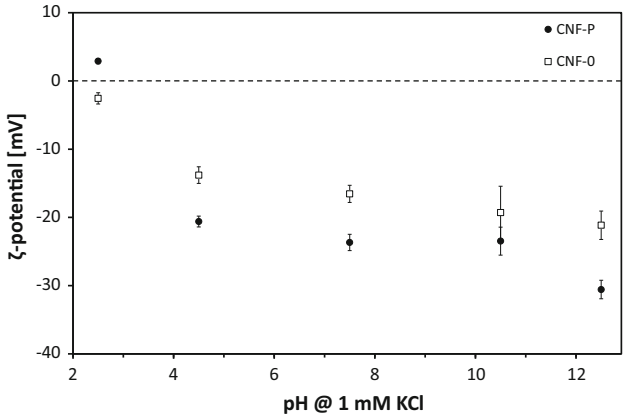

Fig. 1 ζ-Potential of CNF-P and CNF-0 as function of pH

in equal amounts (25 gsm CNF-P and 25 gsm CNF-0, respectively), thus ensuring equal amounts of phosphate groups within 25 gsm CNF-P and 50 gsm CNF-H nanopapers. Furthermore, a double-layer nanopaper was developed, for we hypothesized that the adsorption efficiency of functional groups located on the surface of a nanopaper is higher than those of functional groups in the bulk of a nanopaper. Therefore, a thin layer (10 gsm) of CNF-P was deposited onto a CNF-0 (40 gsm) support, termed "CNF-P top". In addition, for comparison reasons, nanopapers from unmodified CNF-0 with a grammage of 25 gsm gsm, corresponding to a thickness of 25 µm, were prepared according to the same principal protocol.

In nanopapers from pure phosphorylated CNF-P (Fig. 2 left) and hybrid nanopapers made from mixtures of phosphorylated and unmodified CNF (Fig. 2 right), a homogeneous network of nanofibrils was formed. Differences could be observed regarding the alignment of the fibrils. Whereas in CNF-H nanopapers fibrils appear to align over larger distances, in CNF-P nanopapers it seems that due to repulsive forces caused by the negatively charged phosphate groups a more chaotic network has been formed.

The surface charge of adsorption materials most prominently affects their effectiveness. Information regarding type of moieties present and their relative concentrations on a materiaĺs surface is provided by its ζ-potential. Additionally, as cleavage of functional groups at enhanced temperatures might have taken place during the nanopaper production process, the ζ-potential provides information about the type and concentration of functional groups. The ζ-potential of the nanopapers as function of pH in a 1 mol L^{-1} KCl electrolyte was measured for CNF-P (top), CNF-H and CNF-0 nanopapers (Fig. 3).

As expected, unmodified CNF-0 nanopapers exhibited negative ζ-potential over the whole pH range examined, attributed to the presence of a small amount of carboxyl groups, such as uronic acids, originating from residual hemicelluloses in the pulp, which are available to cellulose oxidation during the pulping operation (Olszewska et al. 2011). Just as for CNF-0 nanofibrils, the ζ-potential of CNF-0 nanopapers increased with decreasing pH value, with an extrapolated iep of pH 2. Phosphorylated nanopapers exhibited negative ζ-potential at pH > 4 as well, but on a lower level with a plateau at around −60 mV. This was due to the introduction of acidic phosphate groups that have been grafted to the surface of the cellulose nanofibrils. Because of this very low ζ-potential, adsorption of heavy metal ions such as Cu^{2+} on the negatively charged surface of the nanofibrils should be improved. Similar to the ζ-potential of CNF-P fibrils, at pH 3.5 charge reversal takes place for CNF-P

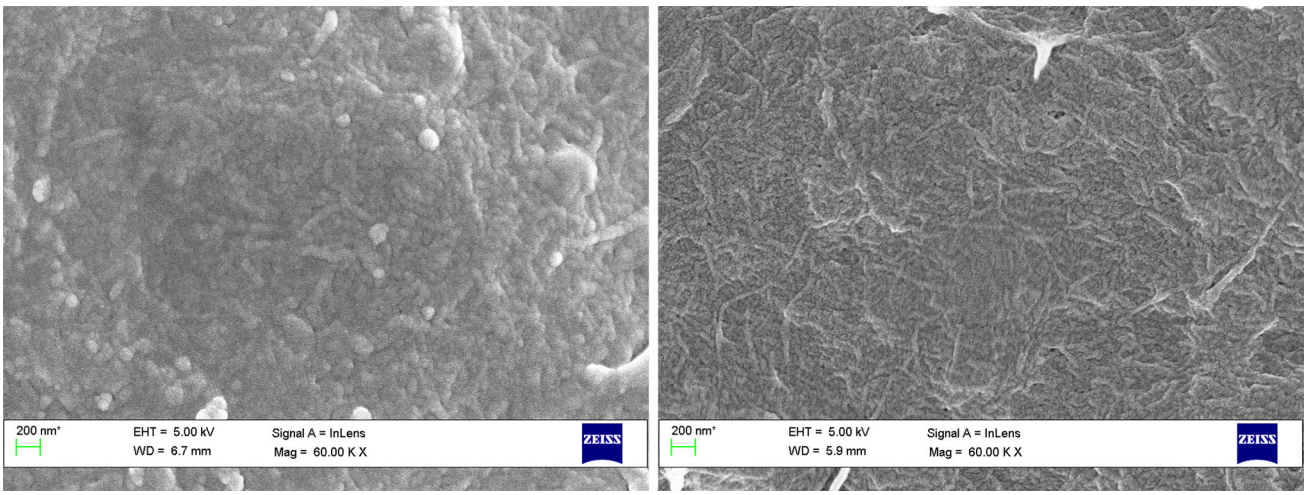

Fig. 2 SEM images of CNF-P nanopapers (*left*) with 25 gsm/25 µm thickness and CNF-H nanopapers (*right*) with 50 gsm/50 µm thickness (magnification: ×60,000)

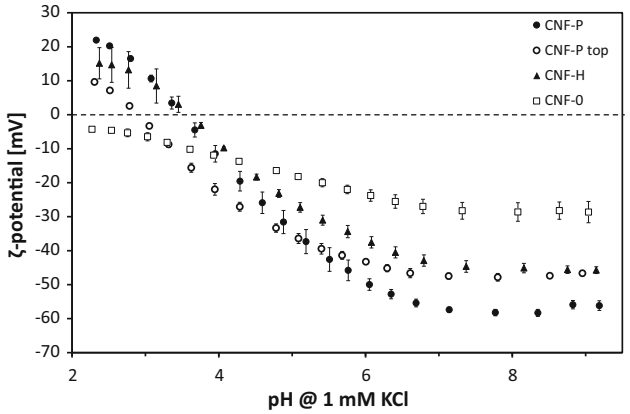

Fig. 3 ζ-Potential of CNF-P (top), CNF-0 and CNF-H nanopapers as function of pH

nanopapers. Hybrid nanopapers, containing both modified CNF-P and unmodified CNF-0, exhibited a ζ-potential that reflects the average of CNF-P and CNF-0. A plateau at around −45 mV, right in between −60 mV for CNF-P and −30 mV for CNF-0 nanopapers, respectively, was measured. The iep is at pH 3.5 just as for CNF-P. Thus, copper adsorption should still be feasible but presumably at a lower level as for pure CNF-P but higher compared to CNF-0. Interestingly, for CNF-P top, the ζ-potential is higher at higher pH as compared to CNF-P, similar to CNF-H, demonstrating the influence of the CNF-0 support onto the ζ-potential. In addition, starting from pH 5 and below, the ζ-potential is lower as compared to CNF-P and also the iep is lowered from pH 3.5 to 3.0.

Tensile properties of nanopapers

In order to evaluate the feasibility of the nanopapers in real filtration experiments, mechanical properties were determined by tensile tests. The results for tensile strength, Young's modulus and strain to failure are summarized for all nanopapers in Table 1 compared to a conventional filter paper VWR 413.

The pure CNF-P nanopaper was found to be the stiffest but also most brittle nanopaper. It exhibited the highest Young's modulus but also lowest strain to failure and tensile strength. This can be explained by repulsion of introduced phosphate groups that render the nanopaper brittle. Opposed to that the completely unmodified CNF-0 nanopaper exhibited a very high tensile strength and strain to failure, which are comparable to conventional nanopapers (Lee et al. 2012). As one would expect, mixtures of CNF-0 and CNF-P fibrils in CNF-H nanopapers and layered structures, such as in CNF-P top nanopapers, exhibited mechanical properties in between pure CNF-0 and CNF-P nanopapers. Compared to conventional, commercially available filter papers, all of the nanopapers showed superior mechanical behaviour. Thus, it is to be expected that the nanopapers are capable of readily withstanding mechanical stresses experienced during filtration experiments.

Nanopaper permeance and copper adsorption performance

In order to quantify the performance of membranes, usually two parameters, the permeance and the rejection of pollutants, are analysed. In this study, the rejection was expressed by the adsorption of copper ions on the nanopaper ion-exchanger. The permeance (P) was measured using deionized water in a dead-end cell. As P is very prone to be varying over time, the equilibrium P had to be established. To do so, the permeance of nanopapers was tested until it did not change more than 1 % during one hour. The results of these measurements are presented for all types of nanopapers in Fig. 4.

The 25 gsm CNF-P nanopapers exhibited almost the same P as 50 gsm CNF-H nanopapers of about 2 L m^{-2} h^{-1} MPa^{-1}. This showed that the introduction of phosphate groups reduces the permeance of nanopapers. This result was confirmed by the permeance for pure 25 gsm CNF-0 nanopapers, which was two times higher as compared to the 25 gsm CNF-P nanopapers. This phenomenon is possibly due to the fact that the modified CNF fibrils with a more negative ζ-potential as compared to CNF-0 (see Fig. 1) are better dispersed in the CNF pulp, and therefore, after filtration the papers consist of fewer large aggregates

Table 1 Tensile properties of CNF-0, CNF-P (top) and CNF-H nanopapers compared to filter paper VWR 413: tensile strength σ (MPa), Young's modulus E (GPa) and strain to failure ε (%)

Nanopaper	Tensile strength σ (MPa)	Young's modulus E (GPa)	Strain to failure ε (%)
CNF-P	51.4	8.7	0.80
CNF-P top	89.0	6.1	3.19
CNF-H	95.3	7.1	1.73
CNF-0	120.3	6.3	5.06
Filter paper	31.6	1.9	2.45

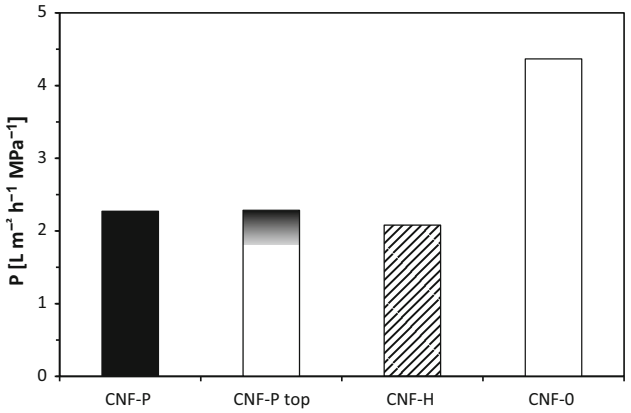

Fig. 4 Stable permeance of CNF-P (top), CNF-0 and CNF-H nanopapers

resulting in bigger pores. The permeance of nanopapers was thus found to be in the range of commercial reverse osmosis membranes, which are usually required to tackle metal ions in membrane processes.

The utility of phosphorylated CNF nanopapers as adsorption membrane for the continuous removal of copper ions from aqueous solutions was demonstrated by filtration experiments. Cellulose nanofibrils, in particular those modified with phosphate groups, have already been demonstrated to adsorb heavy metal ions such as copper ions in static experiments with incubation times of several hours (Božič et al. 2014; Liu et al. 2014, 2015). Yet, in real-time filtration experiments, the contact time between adsorbent and adsorbate is only seconds or even fractions of seconds, potentially allowing for a much faster and thus more efficient process. Consequently, dynamic adsorption experiments were performed to explore the feasibility of copper adsorption onto modified CNF for these short contact times.

A solution of copper nitrate in deionized water at a concentration of 1 mmol L^{-1}, equivalent to 63.5 mg Cu(II) L^{-1}, corresponding to strongly copper contaminated water, similar to effluents from mirror industries (Liu et al. 2015), was used to determine dynamic adsorption characteristics of CNF-P nanopapers. Since batch adsorption tests (Božič et al. 2014) showed only limited heavy metal adsorption by CNF-0, CNF-0 nanopapers were not tested regarding their dynamic copper adsorption performance. CNF-P (top) and CNF-H nanopapers, respectively, were installed in a dead-end cell, and the copper solution was passed through and permeate fractions were collected. Figure 5(left) shows a photograph of a CNF-P top nanopaper after filtration tests. A turquois haze on the surface of the nanopaper shows that the surface of the nanopaper was loaded with Cu(II) ions. This demonstrates the capability of phosphorylated nanopapers for copper removal. Moreover, simply washing the nanopapers with 0.1 M H_3PO_4 (Fig. 5 right) allows to regenerate the nanopaper ion-exchanger; the adsorbed copper was removed and the nanopaper ion-exchanger can be reused.

The copper concentration of each permeate fraction was determined by ICP-OES, and the amount of copper that has been removed from the particular effluent was calculated. The amount of adsorbed copper has then been related to the active membrane area used and plotted against the permeate volume (Fig. 6).

Apparently, the initial slopes of the curves are almost identical for CNF-P and CNF-H and slightly increased for CNF-P top, whereby in the presence of equal concentrations of Ca^{2+} and Cu^{2+} ions the copper adsorption was influenced only to a minor extent. In the latter case, at first hardly any difference was found but the overall copper adsorption capacity was slightly reduced. The initial slopes correspond to the primary adsorption of copper onto the surface of the nanopaper and suggest that phosphate groups on the surface of a nanopaper contribute more to copper adsorption than phosphate groups on fibrils located in the

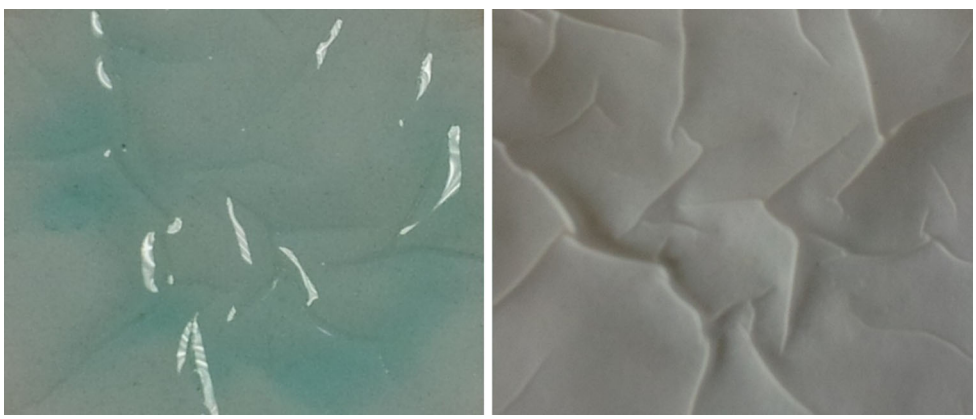

Fig. 5 Image of a CNF-P top nanopaper after adsorption tests (*left*). Adsorbed copper ions can be easily perceived as turquois haze on the surface of the nanopaper. Image of the same CNF-P top nanopaper after treatment with 0.1 M H_3PO_4 to desorb the copper ions (*right*)

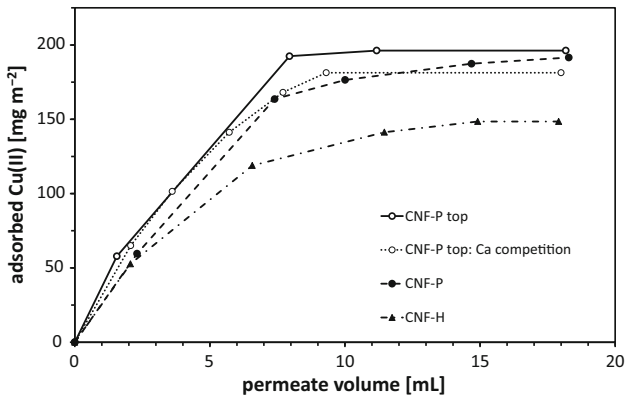

Fig. 6 Mass of adsorbed copper per unit filtration area versus permeate volume for CNF-P (top) (with/without Ca competition) and CNF-H. The *error* of each individual data point corresponds to the *error* of the experiment which was equal to 2 %

bulk of the nanopaper. When saturation of the nanopaper was reached, the curve levelled off. The saturation level quantifies the maximum adsorption capacity of the ion-exchange nanopapers. This value was obviously approximately the same for CNF-P (190 mg m^{-2}) and CNF-P top (195 mg m^{-2}) nanopapers and significantly higher than for CNF-H (150 mg m^{-2}). This situation was explained by the higher number of phosphate groups on the surface of nanopapers made purely from CNF-P or having a thin layer of CNF-P on top, respectively. Thus, apparently it is not the total mass of modified CNF-P in the nanopaper that is responsible for efficient copper adsorption. Rather the concentration of phosphate groups on fibrils located on the surface of the nanopaper dominates adsorption of copper, thus influencing the amount of copper that can be removed. This observation also reflects the results from ζ-potential measurements (Fig. 3). This was due to a greater accessibility of phosphate groups on fibrils located on the nanopaper surface compared to those on fibrils buried in the bulk of the nanopapers.

Table 2 Adsorption capacity for CNF-P, CNF-H and CNF-P top (virgin, with competing Ca and after regeneration) nanopapers

Nanopaper	Adsorption capacity (mg g^{-1})
CNF-P	7.7
CNF-H	5.9
CNF-P top	19.6
CNF-P top: calcium competition	18.1
CNF-P top: after regeneration	19.4

The level of saturation of copper adsorbed on the nanopapers per unit area is a measure for the total quantity of copper that can be adsorbed. Ultimately, the adsorption capacity, i.e. the amount of milligram copper per gram active adsorption agent, in this case phosphorylated CNF-P, was computed from the amount of copper adsorbed by the nanopaper at the saturation level (Table 2). These results confirm again the hypothesis that CNF-P on the surface of the nanopapers contributed more to the removal of copper from aqueous solutions. CNF-P top, which contains only a 10 gsm layer of phosphorylated CNF deposited on a CNF-0 substrate, was capable of adsorbing almost 20 mg copper per g CNF-P. This was over two times more than a pure CNF-P nanopaper is capable of and more than three times of what a nanopaper made from a mixture of CNF-P and CNF-0 was able to adsorb. The lower value of CNF-H nanopapers, as compared to CNF-P nanopapers, even though both types of nanopapers contain equal amounts of phosphorylated CNF, could be explained by the fact that in CNF-H a lower amount of modified CNF is located on the surface of the nanopaper, where presumably higher adsorption efficiency can be achieved.

The results of adsorption capacities of CNF-P nanopapers are comparable to adsorption capacities of other biosorbents from industrial/agricultural residues, whereby particularly CNF-P top nanopapers outperform many of them (Bilal et al. 2013; Titi and Bello 2015). However, the adsorption efficiency is by far higher as contact times of only a couple of seconds are required, whereas for batch-wise adsorption usually contact times of several hours are applied. Unfortunately, adsorption capacities of state-of-the-art commercially available adsorbers could not yet be achieved (Fu and Wang 2011), which is due to the relatively low amount of phosphate groups in the CNF-P grade used (18.6 mmol kg^{-1}). Nevertheless, if it becomes possible to prepare CNF with higher degrees of surface modification, increased adsorption capacities are anticipated (Kokol et al. 2015; Liu et al. 2015). It was also found that the presence of equal concentrations of Ca^{2+} and Cu^{2+} ions resulted in reducing the copper adsorption capacity by less than ten per cent. Ultimately, regenerated nanopapers, achieved by washing with phosphoric acid, exhibited only a marginally lower adsorption capacity.

Conclusion

Cellulose nanofibrils were modified with phosphate groups by reacting CNF derived from cellulose sludge, a waste stream from paper industries, with phosphoric acid. Success of the modification reaction was confirmed by conductometric titration and zeta-potential measurements. Phosphorylated CNF nanopapers, intended to be used as ion-exchange nanopapers for the capture of copper ions, were manufactured via a papermaking process. CNF-P nanopapers exhibited lower permeance as compared to unmodified CNF nanopapers. The nanopaper ion-exchangers were demonstrated to be able to adsorb copper ions in dynamic filtration experiments, i.e. while water containing copper ions was passing the nanopapers. It was found that nanopapers were able to adsorb copper from aqueous solutions up to 200 mg per one m^2 filtration area equivalent to almost 20 mg copper per one g phosphorylated CNF. Another result of this study was that phosphate groups on the surface of the nanopaper apparently contribute more to the overall copper adsorption than functional groups within the bulk of the nanopapers. Furthermore, we demonstrated that, in analogy to conventional ion-exchangers, our nanopapers could be regenerated and reused without significant loss in adsorption capacity. Moreover, the adsorption capacity for copper was reduced by only ten per cent when calcium ions were present in the same concentration. It can be summarized that nanopapers comprising phosphorylated nanofibrils are efficient as membranes for copper removal from contaminated water via electrostatic interactions. The conclusion can be drawn that a thin layer of modified CNF on the surface of a paper results in highest efficiency concerning permeance and copper adsorption.

Acknowledgments Open access funding provided by University of Vienna. The authors greatly acknowledge the funding provided by EU FP7 project NanoSelect (Grant No. 280519) and Processum for providing the raw materials. T.K. thanks the Thailand Research Fund through the Royal Golden Jubilee PhD Program (Grant No. PHD/0137/2554) for financial support.

References

Akar ST, Akar T, Kaynak Z, Anilan B, Cabuk A, Tabak Ö, Demir TA, Gedikbey T (2009) Removal of copper(II) ions from synthetic solution and real wastewater by the combined action of dried trametes versicolor cells and montmorillonite. Hydrometallurgy 97:98–104

Araya M, McGoldrick MC, Klevay LM, Strain JJ, Robson P, Nielsen F, Olivares M, Pizarro F, Johnson L, Poirier KA (2001) Determination of an acute no-observed-adverse-effect level (NOAEL) for copper in water. Regul Toxicol Pharm 34:137–145

Bansal M, Mudhoo A, Garg VK, Singh D (2014) Preparation and characterization of biosorbents and copper sequestration from simulated wastewater. Int J Environ Sci Technol 11:1399–1412

Bhatnagar A, Sillanpää M (2011) A review of emerging adsorbents for nitrate removal from water. Chem Eng J 168:493–504

Bilal M, Shah JA, Ashfaq T, Gardazi SMH, Tahir AA, Pervez A, Haroon H, Mahmood Q (2013) Waste biomass adsorbents for copper removal from industrial wastewater—a review. J Hazard Mater 263(2):322–333

Božič M, Liu P, Mathew A, Kokol V (2014) Enzymatic phosphorylation of cellulose nanofibers to new highly-ions adsorbing, flame-retardant and hydroxyapatite-growth induced natural nanoparticles. Cellulose 21:2713–2726

Camarillo R, Llanos J, García-Fernández L, Pérez Á, Cañizares P (2010) Treatment of copper (II)-loaded aqueous nitrate solutions by polymer enhanced ultrafiltration and electrodeposition. Sep Purif Technol 70:320–328

Castaldi P, Silvetti M, Garau G, Demurtas D, Deiana S (2015) Copper(II) and lead(II) removal from aqueous solution by water treatment residues. J Hazard Mater 283:140–147

C.D.A. (2015) Annual data 2015: copper supply and consumption—1994–2014. http://www.copper.org/resources/market_data/pdfs/annual_data.pdf. Accessed 12 Feb 2016

Chen Q, Luo Z, Hills C, Xue G, Tyrer M (2009) Precipitation of heavy metals from wastewater using simulated flue gas: sequent additions of fly ash, lime and carbon dioxide. Water Res 43:2605–2614

Cretescu I, Soreanu G, Harja M (2015) A low-cost sorbent for removal of copper ions from wastewaters based on sawdust/fly ash mixture. Int J Environ Sci Technol 12:1799–1810

Davis TA, Volesky B, Mucci A (2003) A review of the biochemistry of heavy metal biosorption by brown algae. Water Res 37:4311–4330

Deng PY, Liu W, Zeng BQ, Qiu YK, Li LS (2013) Sorption of heavy metals from aqueous solution by dehydrated powders of aquatic plants. Int J Environ Sci Technol 10:559–566

European-Comission (2003) Opinion of the scientific committee on food on the tolerable upper intake level of copper (scf/cs/nut/upplev/57 final). http://ec.europa.eu/food/fs/sc/scf/out176_en.pdf. Accessed 12 Nov 2014

Feitoza NC, Gonçalves TD, Mesquita JJ, Menegucci JS, Santos M-KMS, Chaker JA, Cunha RB, Medeiros AMM, Rubim JC, Sousa MH (2014) Fabrication of glycine-functionalized maghemite nanoparticles for magnetic removal of copper from wastewater. J Hazard Mater 264:153–160

Fraga CG (2005) Relevance, essentiality and toxicity of trace elements in human health. Mol Aspects Med 26:235–244

Fu F, Wang Q (2011) Removal of heavy metal ions from wastewaters: a review. J Environ Manag 92:407–418
Gupta VK (1998) Equilibrium uptake, sorption dynamics, process development, and column operations for the removal of copper and nickel from aqueous solution and wastewater using activated slag, a low-cost adsorbent. Ind Eng Chem Res 37:192–202
Guthrie JP (1977) Hydration and dehydration of phosphoric acid derivatives: free energies of formation of the pentacoordinate intermediates for phosphate ester hydrolysis and of monomeric metaphosphate. J Am Chem Soc 99:3991–4001
Hasani M, Cranston ED, Westman G, Gray DG (2008) Cationic surface functionalization of cellulose nanocrystals. Soft Matter 4:2238–2244
Henriksson M, Berglund LA, Isaksson P, Lindström T, Nishino T (2008) Cellulose nanopaper structures of high toughness. Biomacromolecules 9:1579–1585
Hokkanen S, Repo E, Sillanpää M (2013) Removal of heavy metals from aqueous solutions by succinic anhydride modified mercerized nanocellulose. Chem Eng J 223:40–47
Huang S-Y, Fan C-S, Hou C-H (2014) Electro-enhanced removal of copper ions from aqueous solutions by capacitive deionization. J Hazard Mater 278:8–15
Jain R, Dominic D, Jordan N, Rene ER, Weiss S, van Hullebusch ED, Hübner R, Lens PNL (2016) Preferential adsorption of cu in a multi-metal mixture onto biogenic elemental selenium nanoparticles. Chem Eng J 284:917–925
Jin S, Chen Y, Liu M (2013) Nanocellulose applications in environmental protection. Adv Mater Res 662:198–201
Jonoobi M, Mathew AP, Oksman K (2012) Producing low-cost cellulose nanofiber from sludge as new source of raw materials. Ind Crop Prod 40:232–238
Karim Z, Mathew AP, Grahn M, Mouzon J, Oksman K (2014) Nanoporous membranes with cellulose nanocrystals as functional entity in chitosan: removal of dyes from water. Carbohydr Polym 112:668–676
Klemm D, Kramer F, Moritz S, Lindstroem T, Ankerfors M, Gray D, Dorris A (2011) Nanocelluloses: a new family of nature-based materials. Angew Chem Int Ed 50:5438–5466
Kokol V, Božič M, Vogrinčič R, Mathew AP (2015) Characterisation and properties of homo- and heterogenously phosphorylated nanocellulose. Carbohydr Polym 125:301–313
Komkiene J, Baltrenaite E (2016) Biochar as adsorbent for removal of heavy metal ions [cadmium(II), copper(II), lead(II), zinc(II)] from aqueous phase. Int J Environ Sci Technol 13:471–482
Kongsricharoern N, Polprasert C (1995) Electrochemical precipitation of chromium (Cr^{6+}) from an electroplating wastewater. Water Sci Technol 31:109–117
Lambert A, Drogui P, Daghrir R, Zaviska F, Benzaazoua M (2014) Removal of copper in leachate from mining residues using electrochemical technology. J Environ Manag 133:78–85
Lee K-Y, Tammelin T, Schulfter K, Kiiskinen H, Samela J, Bismarck A (2012) High performance cellulose nanocomposites: comparing the reinforcing ability of bacterial cellulose and nanofibrillated cellulose. ACS Appl Mater Interfaces 4:4078–4086
Liu P, Sehaqui H, Tingaut P, Wichser A, Oksman K, Mathew A (2014) Cellulose and chitin nanomaterials for capturing silver ions (Ag^{+}) from water via surface adsorption. Cellulose 21:449–461
Liu P, Borrell PF, Božič M, Kokol V, Oksman K, Mathew AP (2015) Nanocelluloses and their phosphorylated derivatives for selective adsorption of Ag^{+}, Cu^{2+} and Fe^{3+} from industrial effluents. J Hazard Mater 294:177–185
Mautner A, Lee K-Y, Lahtinen P, Hakalahti M, Tammelin T, Li K, Bismarck A (2014) Nanopapers for organic solvent nanofiltration. Chem Commun 50:5778–5781
Mautner A, Lee K-Y, Tammelin T, Mathew AP, Nedoma AJ, Li K, Bismarck A (2015) Cellulose nanopapers as tight aqueous ultrafiltration membranes. React Funct Polym 86:209–214
Mautner A, Maples HA, Sehaqui H, Zimmermann T, Perez de Larraya U, Mathew AP, Lai CY, Li K, Bismarck A (2016) Nitrate removal from water using a nanopaper ion-exchanger. Environ Sci Water Res Technol 2:117–124
Mejias Carpio IE, Machado-Santelli G, Kazumi Sakata S, Ferreira Filho SS, Rodrigues DF (2014) Copper removal using a heavy-metal resistant microbial consortium in a fixed-bed reactor. Water Res 62:156–166
Olszewska A, Eronen P, Johansson L-S, Malho J-M, Ankerfors M, Lindström T, Ruokolainen J, Laine J, Österberg M (2011) The behaviour of cationic nanofibrillar cellulose in aqueous media. Cellulose 18:1213–1226
Pei A, Butchosa N, Berglund LA, Zhou Q (2013) Surface quaternized cellulose nanofibrils with high water absorbency and adsorption capacity for anionic dyes. Soft Matter 9:2047–2055
Qdais HA, Moussa H (2004) Removal of heavy metals from wastewater by membrane processes: a comparative study. Desalination 164:105–110
Samuelsson C, Björkman B (2014) Chapter 7 - copper recycling. In: Worrell E, Reuter MA (eds) Handbook of recycling. Elsevier, Boston, pp 85–94
Sehaqui H, Liu A, Zhou Q, Berglund LA (2010) Fast preparation procedure for large, flat cellulose and cellulose/inorganic nanopaper structures. Biomacromolecules 11:2195–2198
Sehaqui H, de Larraya U, Liu P, Pfenninger N, Mathew A, Zimmermann T, Tingaut P (2014) Enhancing adsorption of heavy metal ions onto biobased nanofibers from waste pulp residues for application in wastewater treatment. Cellulose 21:2831–2844
Şen A, Pereira H, Olivella MA, Villaescusa I (2015) Heavy metals removal in aqueous environments using bark as a biosorbent. Int J Environ Sci Technol 12:391–404
Shaheen SM, Eissa FI, Ghanem KM, Gamal El-Din HM, Al Anany FS (2013) Heavy metals removal from aqueous solutions and wastewaters by using various byproducts. J Environ Manag 128:514–521
Shannon MA, Bohn PW, Elimelech M, Georgiadis JG, Marinas BJ, Mayes AM (2008) Science and technology for water purification in the coming decades. Nature 452:301–310
Suflet DM, Chitanu GC, Desbrières J (2010) Phosphorylated polysaccharides. 2. Synthesis and properties of phosphorylated dextran. Carbohydr Polym 82:1271–1277
Tegoni M, Valensin D, Toso L, Remelli M (2014) Copper chelators: chemical properties and bio-medical applications. Curr Med Chem 21:3785–3818
Titi OA, Bello OS (2015) An overview of low cost adsorbents for copper(II) ions removal. J Biotechnol Biomater 5:117
Ujang Z, Anderson GK (1996) Application of low-pressure reverse osmosis membrane for Zn^{2+} and Cu^{2+} removal from wastewater. Water Sci Technol 34:247–253
Wan Ngah WS, Endud CS, Mayanar R (2002) Removal of copper(II) ions from aqueous solution onto chitosan and cross-linked chitosan beads. React Funct Polym 50:181–190
WHO (2004) Copper in drinking-water (who/sde/wsh/03.04/88). http://www.who.int/water_sanitation_health/dwq/chemicals/copper.pdf. Accessed 12 Feb 2016

Yu X, Tong S, Ge M, Wu L, Zuo J, Cao C, Song W (2013a) Adsorption of heavy metal ions from aqueous solution by carboxylated cellulose nanocrystals. J Environ Sci 25:933–943

Yu X, Tong S, Ge M, Wu L, Zuo J, Cao C, Song W (2013b) Synthesis and characterization of multi-amino-functionalized cellulose for arsenic adsorption. Carbohydr Polym 92:380–387

Zamani HA, Rajabzadeh G, Firouz A, Ganjali MR (2007) Determination of copper(II) in wastewater by electroplating samples using a pvc-membrane copper(II)-selective electrode. J Anal Chem 62:1080–1087

Zhu Q, Li Z (2015) Hydrogel-supported nanosized hydrous manganese dioxide: synthesis, characterization, and adsorption behavior study for Pb^{2+}, Cu^{2+}, Cd^{2+} and Ni^{2+} removal from water. Chem Eng J 281:69–80